Free-carrier-driven spatiotemporal dynamics in amplifying silicon waveguides

Roy, Samudra; Marini, Andrea; Biancalana, Fabio

Published in:
Physical Review A (Atomic, Molecular, and Optical Physics)

DOI:
10.1103/PhysRevA.89.053827

Publication date:
2014

Free-carrier-driven spatiotemporal dynamics in amplifying silicon waveguides

Samudra Roy,[1,2] Andrea Marini,[1] and Fabio Biancalana[1,3]
[1]*Max Planck Institute for the Science of Light, Günther-Scharowsky-Straße 1, 91058 Erlangen, Germany*
[2]*Department of Physics, Indian Institute of Technology, Kharagpur 721302, India*
[3]*School of Engineering and Physical Sciences, Heriot-Watt University, Edinburgh EH14 4AS, United Kingdom*
(Received 20 January 2014; published 23 May 2014)

We theoretically investigate the free-carrier-induced spatiotemporal dynamics of continuous waves in silicon waveguides embedded in an amplifying medium. Optical propagation is governed by a cubic Ginzburg-Landau equation coupled with an ordinary differential equation accounting for the free-carrier dynamics. We find that, owing to free-carrier dispersion, continuous waves are modulationally unstable in both anomalous and normal dispersion regimes and chaotically generate unstable accelerating pulses.

DOI: 10.1103/PhysRevA.89.053827 PACS number(s): 42.65.Tg, 42.65.Sf, 42.65.Wi

I. INTRODUCTION

Silicon photonics is a well-established area of research aiming at exploiting silicon as a photonic component for the engineering of integrated optoelectronic devices. The extraordinary optical properties of Si open up possibilities for novel miniaturized applications, ranging from optical interconnection to biosensing [1,2]. In the mid-infrared, Si has a high refractive index ($n \simeq 3.5$) and negligible linear extinction. However, in the range $1\ \mu\text{m} < \lambda_0 < 2.2\ \mu\text{m}$, two-photon absorption (TPA) is relevant and is responsible for high nonlinear extinction [3]. Owing to the high refractive index, light can be tightly localized in subwavelength Si-based waveguides [4], which tremendously enhance nonlinear processes [5], including TPA that damps optical propagation and limits the efficiency of Si-based photonic components [6]. As a consequence of TPA, pairs of photons with total energy greater than the Si band gap ($E_g \approx 1.12$ eV) are absorbed, and electrons are excited to the conduction band modifying the Si optical response [7]. In this interesting and rather unexplored operating regime, free carriers (FCs) directly interact with the optical field and introduce novel nonlinear effects [8]. A quite similar scenario happens in gas-filled hollow core photonic crystal fibers (HCPCFs) in the ionization regime, where accelerating solitons [9] and universal modulational instability [10] have been recently observed. In this case, the free plasma generated through ionization is responsible for an intense *blueshift* of several hundreds of nanometers of the optical pulse [11]. This tremendous dynamics occurs on a much smaller scale (blueshift of a few nanometers) in Si-based waveguides [8] because of the intimate presence of TPA, which is responsible for both the creation of FCs and for damping. In principle, losses can be reduced in hybrid slot waveguides [12], but in this case the extraordinary effects ensuing from FC dynamics are also reduced accordingly.

An alternative strategy for overcoming losses consists of embedding Si waveguides in gaining media. In this context, amplification schemes based on III–V semiconductors [13], rare-earth-ion-doped dielectric thin films [14], and erbium-doped waveguides [15] have been proposed and practically realized. The paradigm model for describing optical propagation in amplifying waveguides is represented by the cubic Ginzburg-Landau (GL) equation, which governs a wide range of dissipative phenomena [16,17]. In general, GL systems are rich in nature and exhibit some peculiar features, e.g., chaos and pattern formation [18,19]. In contrast to the case of conventional Kerr solitons arising from the balance between nonlinearity and dispersion [20], localized stationary solutions of GL systems, namely, *dissipative solitons,* result from the exact compensation of gain and loss [21]. In a recent work, we investigated the FC-induced dynamics of dissipative solitons in Si-based amplifying waveguides, demonstrating the self-frequency soliton blueshift [22].

In this paper, we theoretically investigate the propagation of continuous waves (cw's) in a silicon-on-insulator (SOI) waveguide embedded in erbium-doped amorphous aluminum oxide (Al_2O_3:Er^+). Owing to the externally pumped active inclusions, small optical waves are exponentially amplified, and instability develops until the nonlinear gain saturation comes into play, counterbalancing the linear amplification. Taking full account of FC generation and recombination, we calculate the stationary nonlinear cw's of the system, and we investigate their stability. We find that, analogous to gas-filled HCPCFs [10], stationary cw's are universally unstable in both normal and anomalous dispersion regimes. However, due to the inherent nonconservative nature of our system, modulational instability (MI) does not generate a shower of solitons as in Ref. [10] but an *accelerating chaotic state*. This scenario ensues from the presence of unstable dissipative solitons, which constitute the strange attractor of the system [18]. Every subpulse generated through MI is accelerated by the FC dispersion and experiences self-frequency blueshift. In turn, the overall dynamics accelerates in the temporal domain and blueshifts in the frequency domain. This paper is organized as follows. In Sec. II we describe the geometry of the system and the governing equations. In Sec. III we calculate the nonlinear stationary cw modes that result from the thorough balance between the gain provided by externally pumped two-level atoms and Si TPA. In Sec. IV we analytically and numerically study MI of cw's. Analytical calculations predict universal MI and accelerating chaos, which is confirmed by numerical simulations.

II. MODEL

We consider a SOI waveguide with lateral dimensions $h = w = 525$ nm surrounded by Al_2O_3:Er^+, whose gain bandwidth is of the order of 100 nm around the carrier wavelength $\lambda \simeq 1540$ nm. In principle, other gain schemes involving the use of semiconductor active materials can be considered, and the gain

bandwidth can be increased accordingly [23]. Without any loss of generality, we assume that the SOI waveguide is fabricated along the $[\bar{1}10]$ direction and on the $[110]\times[001]$ surface. In this case, stimulated Raman scattering (SRS) does not occur for quasi-TM modes [7]. Initially neglecting gain of the external medium, Si nonlinearity, and FC generation, we have numerically calculated the linear quasi-TM mode $\mathbf{e}(\mathbf{r}_\perp)$, its dispersion $\beta_0(\omega_0)$, and the effective area by using COMSOL [24]. At $\lambda_0 = 1550$ nm, we then found that the second-order group velocity dispersion (GVD) coefficient is $\beta_2 \simeq -2$ ps^2/m and the effective area is $A_{\rm eff} \simeq 0.145\ \mu$m^2. Nonlinear pulse propagation can be modeled within the slowly varying envelope approximation (SVEA) by taking the ansatz for the electric field $\mathbf{E}(\mathbf{r},t) = \mathrm{Re}[A(z,t)\mathbf{e}(\mathbf{r}_\perp)e^{i\beta_0 z - i\omega_0 t}]$, where $A(z,t)$ is the pulse envelope, $\mathbf{e}(\mathbf{r}_\perp)$ is the linear mode profile, $\omega_0 = 2\pi c/\lambda_0$ is the carrier angular frequency, c is the speed of light in vacuum, and β_0 is the linear propagation constant. We approximate the external gaining medium as a two-level system, which is characterized by a Lorentzian spectral distribution of gain around the carrier angular frequency ω_0: $G(\Delta\omega) = g_0/(1+\Delta\omega^2 T_2^2)$, where g_0 is the dimensionless gain peak, $T_2 \simeq 40$ fs is the dephasing time of Al_2O_3:Er^+, and $\Delta\omega = \omega - \omega_0$ [25]. For small detuning $\Delta\omega \ll \omega_0$, the spectral gain distribution can be approximated by $G(\Delta\omega) \simeq g_0 - g_2\Delta\omega^2 T_2^2$. FCs affect the optical propagation by means of two mechanisms: FC-induced dispersion (FCD) and absorption (FCA). Following the theoretical approach developed in Refs. [26–28], the propagation equation for the optical envelope is found as the solvability condition of the first-order multiscale expansion of the full vectorial Maxwell equations, which reduce to a Ginzburg-Landau equation. In addition, owing to the presence of FCD and FCA in Si-based waveguides, optical propagation is coupled with a nonlinear first-order equation for the generation of FCs, as demonstrated in Refs. [4,7,29]:

$$i\partial_\xi u - \frac{s}{2}\partial_\tau^2 u - igu - ig_2\partial_\tau^2 u \tag{1}$$

$$+(1+iK)|u|^2 u + (i/2-\mu)\phi_c u = 0,$$

$$\frac{d\phi_c}{d\tau} = \theta_c|u|^4 - \frac{\phi_c}{\tau_c}, \tag{2}$$

where u represents the optical envelope and ϕ_c is the free-carrier density. Time duration ($\tau = t/t_0$) and the propagation coordinate ($\xi = z/L_{\rm D}$) are normalized to the pulse duration $t_0 = 40$ fs and dispersion length $L_{\rm D} = t_0^2/|\beta_2| = 0.8$ mm, respectively. The envelope amplitude ($u = A/\sqrt{P_0}$) is normalized to the square root of the power $P_0 = \lambda_0 A_{\rm eff}/(2\pi n_2 L_{\rm D}) = 17.88$ W, where $n_2 = 2.5\times10^{-18}$ m^2/W is the Kerr nonlinear coefficient of bulk silicon [30]. In Eq. (1), the parameter $s = \pm1$ represents the sign of the GVD ($s = +1$ for normal dispersion and $s = -1$ for anomalous dispersion), while the parameter $K = \beta_{\rm TPA}\lambda_0/(4\pi n_2) = 0.4$ is the TPA coefficient, where $\beta_{\rm TPA} \simeq 8\times10^{-12}$ m/W is the bulk TPA constant [30]. The parameter $g = g_0 - \alpha$ is the difference between the gain peak power and the linear loss coefficient ($\alpha_l \simeq 0.2$ dB/cm), which is renormalized to the dispersion length ($\alpha = \alpha_l L_{\rm D} = 0.08$). The FC density N_c is normalized to $\phi_c = \sigma N_c L_{\rm D}$, where $\sigma \simeq 1.45\times10^{-21}$m^2 [31]. The parameter $\theta_c = \beta_{\rm TPA}|\beta_2|\sigma\lambda_0^3/(16\pi^3 c\hbar t_0 n_2^2) = 0.02$ accounts for FCA, while $\mu = 2\pi k_c/(\sigma\lambda_0) = 3.77$ accounts for FCD, where $k_c \simeq 1.35\times10^{-27}$ m^3 [30,32]. The characteristic FC recombination time ($t_c = 1$ ns) is also normalized to the initial pulse width: $\tau_c = t_c/t_0 = 2.5\times10^4$. The peak gain g_0 and the gain dispersion $g_2 = g_0 T_2^2$ are the control parameters of our system, as they can be finely tuned by varying the external pumping power used to achieve inversion of the population of two-level atoms embedded in our system. In Table I, we list the parameters used in the following calculations expressed both in physical units and in the normalized dimensionless units that we have adopted. We emphasize that the SOI waveguide used for the calculation of these parameters is characterized by anomalous dispersion ($s = -1$). For the numerical simulations in the normal dispersion regime developed in this paper, we have assumed hypothetically a SOI waveguide with the same physical parameters as listed in Table I except $\beta_2 = +2$ ps^2/m ($s = +1$).

III. NONLINEAR STATIONARY cw MODES

Owing to the externally pumped active inclusions of the dielectric medium surrounding the SOI waveguide, small-amplitude optical waves are amplified if the peak gain g_0

TABLE I. Physical parameters used in our calculations. We considered a SOI waveguide fabricated along the $[\bar{1}10]$ direction and on the $[110]\times[001]$ surface with lateral dimensions $h = w = 525$ nm surrounded by Al_2O_3:Er^+. This waveguide is characterized by anomalous dispersion, accounted for by the coefficient $\beta_2 = -2$ ps^2/m ($s = -1$). For the numerical simulations in the normal dispersion regime developed in this paper, we have assumed hypothetically a SOI waveguide with the physical parameters listed above except $\beta_2 = +2$ ps^2/m ($s = +1$).

Physical Parameter	Physical Quantity	Normalized Dimensionless Value
Initial pulse duration	$t_0 = 40$ fs	$\tau = 1$
Dispersion coefficient	$\beta_2 = \pm2$ ps^2/m	$s = \pm1$
Dispersion length	$L_D = 0.8$ mm	$\xi = 1$
Scaling peak power	$P_0 = 17.88$ W	$\lvert u\rvert^2 = 1$
Nonlinear coefficient	$n_2 = 2.5\times10^{-18}$ m^2/W	1
Linear loss coefficient	$\alpha_l = 0.2$ dB/cm	$\alpha = 0.08$
Two-photon absorption coefficient	$\beta_{TPA} = 8\times10^{-12}$ m/W	$K = 0.4$
Scaling free-carrier density	$(\sigma L_D)^{-1} = 8.62\times10^5\mu$m^{-3}	$\phi_c = 1$
Free-carrier generation rate	$\theta_c/t_0 = 5\times10^{-4}$ fs^{-1}	$\theta_c = 0.02$
Free-carrier recombination time	$t_c = 1$ ns	$\tau_c = 2.5\times10^4$
Free-carrier dispersion coefficient	$\mu/L_D = 4.72$ mm^{-1}	$\mu = 3.77$

overcomes the linear loss α: $g = g_0 - \alpha > 0$. In turn, the vacuum state $u = 0$ is unstable since any small perturbation is amplified. However, as intensity grows, TPA becomes stronger, and for a specific value of the optical amplitude it thoroughly counterbalances linear amplification. Thus, stationary cw's exist only for the particular value of the optical amplitude such that the effects of linear amplification and TPA compensate for each other. This solution can be found by setting the ansatz

$$u = \rho e^{i\eta\xi}, \tag{3}$$

$$\phi_c = \phi_0, \tag{4}$$

where ρ,η are the optical amplitude and propagation constant and $\phi_0 = \theta_c\tau_c\rho^4$ is the stationary number of FCs such that FC generation is exactly compensated for by FC recombination: $d\phi_c/d\tau = 0$. Inserting the ansatz above into Eqs. (1) and (2), one gets

$$\rho^2 = -\epsilon_c + \sqrt{\epsilon_c^2 + 2\rho_0^2\epsilon_c}, \tag{5}$$

$$\eta = \rho^2 + 2\mu K\left(\rho^2 - \rho_0^2\right), \tag{6}$$

where $\epsilon_c = K/(\theta_c\tau_c)$ and $\rho_0^2 = g/K$. In the absence of FCs ($\epsilon_c \to \infty$), the mode amplitude ρ converges to ρ_0, which coincides with the cw mode amplitude of the uncoupled cubic GL equation. Equation (6) constitutes the dispersion relation of nonlinear stationary waves above threshold ($g > 0$). The threshold condition can be easily found experimentally, as the threshold crossover is typically accompanied by the signature of spectral narrowing [33]. Below threshold ($g < 0$), nonlinear stationary modes of Eqs. (1) and (2) do not exist, as

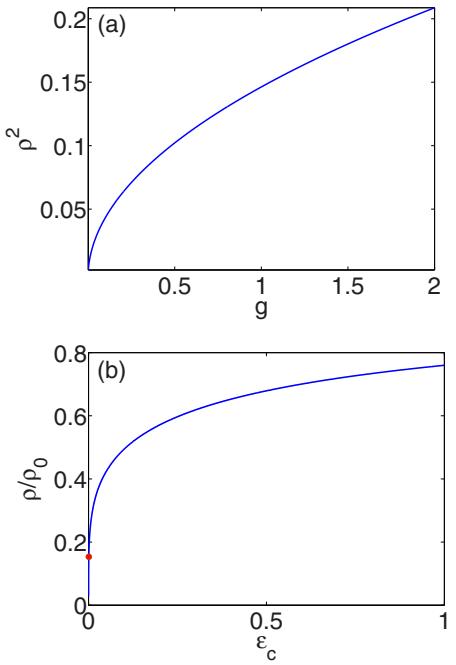

FIG. 1. (Color online) (a) Squared amplitude ρ^2 of the stationary nonlinear cw mode as a function of the effective gain parameter $g = g_0 - \alpha$ given by the difference between the gain peak of the external medium g_0 and the Si loss α. (b) Dependence of the rescaled mode amplitude ρ/ρ_0 on the FC parameter ϵ_c for $g = 1, g_2 = 0.16$. The red dot indicates the exact value of ρ/ρ_0 for the realistic parameters listed in Table I.

the linear gain provided by the externally pumped two-level atoms is not sufficient to overcome the linear loss of Si; in turn, homogeneous waves are damped.

Note that the solution above does not constitute a parametric family, but rather an isolated fixed point, as it generally occurs in dissipative systems [16]. Indeed, there exists a unique optical amplitude and a unique FC density such that the homogeneous mode remains stationary. In Fig. 1(a), the stationary nonlinear cw mode squared amplitude ρ^2 is plotted against the effective gain parameter ($g = g_0 - \alpha$), given by the difference between the external gain and the Si loss. In Fig. 1(b), the mode amplitude rescaled to the GL amplitude (ρ/ρ_0) is plotted against the FC parameter ϵ_c. Note that $\rho \to \rho_0$ in the limit where FCs are not excited ($\epsilon_c \to \infty$). The red dot indicates the exact value of ρ/ρ_0 for $g = 1, g_2 = 0.16$, and the realistic parameters listed in Table I.

IV. MODULATIONAL INSTABILITY

Modulational instability (MI) of the nonlinear cw stationary mode given in Eqs. (5) and (6) can be determined by perturbing it with small time- and space-dependent waves:

$$u = [\rho + a(\tau,\xi)]e^{i\eta\xi}, \tag{7}$$

$$\phi_c = \phi_0 + b(\tau,\xi), \tag{8}$$

where $a(\tau,\xi), b(\tau,\xi)$ are spatiotemporal perturbations of the optical field and of the FC distribution. Plugging the ansatz above in Eqs. (1) and (2) and retaining only linear terms, one achieves the following set of coupled equations for a,b:

$$i\partial_\xi a = (\eta + ig)a + \left(\frac{s}{2} + ig\right)\partial_\tau^2 a \tag{9}$$

$$-(1 + iK)\rho^2(2a + a^*) - \left(\frac{i}{2} - \mu\right)(\phi_0 a + \rho b),$$

$$\frac{db}{d\tau} = 2\theta_c\rho^3(a + a^*) - \frac{b}{\tau_c}. \tag{10}$$

We assume that $a = a_1 e^{\vartheta} + a_2^* e^{\vartheta^*}$, $b = b_0 e^{\vartheta} + b_0^* e^{\vartheta^*}$, where $\vartheta = h\xi + i\Omega\tau$, h is the spatial growth rate of the small periodic perturbations, and Ω is their angular frequency. Note that ϕ_c is real and positive since it represents the number of FCs generated via TPA. Inserting the expressions above for a,b in Eqs. (9) and (10), we achieve a set of algebraic equations for the optical field perturbations a_1,a_2:

$$\begin{bmatrix} ih + F + TL & P + TL \\ P^* + T^*L & -ih + F^* + T^*L \end{bmatrix}\begin{bmatrix} a_1 \\ a_2 \end{bmatrix} = 0, \tag{11}$$

where $P = (1 + iK)\rho^2$, $T = 2\rho^4\theta_c(i/2 - \mu)$, and

$$L = \frac{\tau_c^{-1} - i\Omega}{\tau_c^{-2} + \Omega^2}, \tag{12}$$

$$F = \left(\frac{s}{2} + ig\right)\Omega^2 + 2P - \eta - ig + \left(\frac{i}{2} - \mu\right)\phi_0. \tag{13}$$

Nontrivial solutions can be found by setting the determinant of the coefficient matrix to zero, achieving the instability

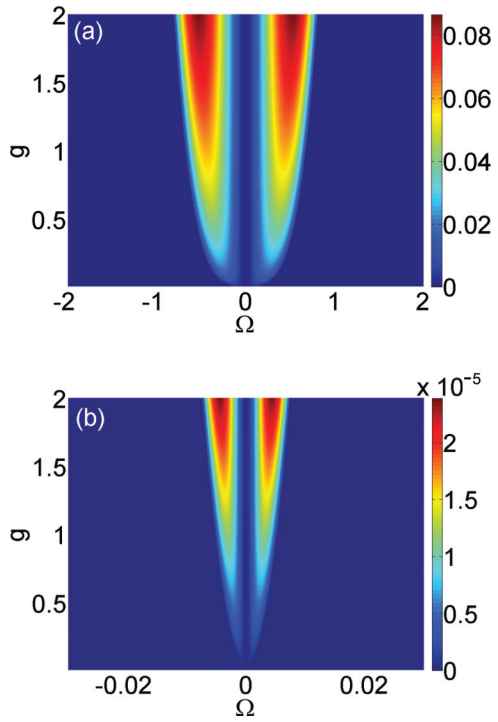

FIG. 2. (Color online) Contour plots for the MI spatial growth rate h as a function of effective gain g and angular frequency Ω for $g_2 = 0.16$ and (a) the anomalous ($s = -1$) and (b) normal ($s = +1$) dispersion regimes. Other parameters used in the calculations are listed in Table I.

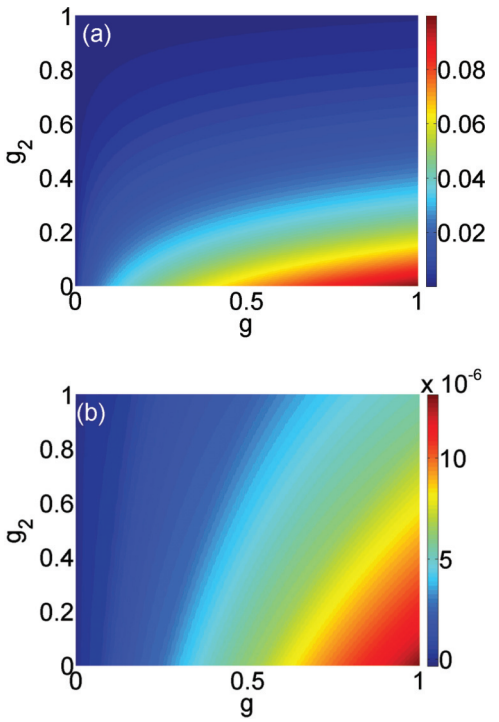

FIG. 3. (Color online) Contour plot of the maximum instability eigenvalue $\max_\Omega h$ as a function of g, g_2 in (a) the anomalous ($s = -1$) and (b) normal ($s = +1$) dispersion regimes. The parameters used in the calculations are listed in Table I.

eigenvalues

$$h_{1,2} = -A_0(\Omega) \pm \sqrt{A_0^2(\Omega) - B_0(\Omega)}, \tag{14}$$

where

$$A_0 = K\rho^2 + g_2\Omega^2 + L\theta_c\rho^4, \tag{15}$$

$$B_0 = \left(\frac{1}{4} + g_2^2\right)\Omega^4 + (2g_2K + s)\rho^2\Omega^2 + 2L\theta_c(g_2 - s\mu)\rho^4\Omega^2. \tag{16}$$

If the real part of h_1 or h_2 is positive, small perturbations are amplified during propagation, giving rise to instability. In Figs. 2(a) and 2(b), we plot the instability parameter $h = \max[\mathrm{Re}h_{1,2}]$ as a function of the effective gain g and angular frequency Ω for anomalous (AD) and normal (ND) dispersion, respectively. The interplay between nonlinear and dispersive effects leads to instability across the central frequency by creating sidebands. Small perturbations with angular frequencies falling within these spectral regions are amplified, and eventually the nonlinear stationary cw mode breaks up into a train of pulses. Owing to the refractive index change induced by FCs, these pulses are accelerated, and we found that the instability eigenvectors are asymmetrically peaked on a blueshifted frequency. Remarkably, FC-induced instability can be observed in the ND regime, analogous to universal plasma-induced instability observed in gas-filled hollow-core photonic crystal fibers [10]. In Figs. 3(a) and 3(b) we have plotted the maximum instability eigenvalue $\max_\Omega h$ as a function of g, g_2 for anomalous and normal dispersion, respectively. Note that in both regimes, the instability parameter increases with gain and is reduced by gain dispersion. While in AD generation of FCs counteracts instability, in ND it is the sole crucial term responsible for its occurrence. Note that also the vacuum background is unstable in supercritical conditions ($g > 0$).

In order to confirm our theoretical predictions we have numerically solved Eqs. (1) and (2) by using split-step fast-Fourier-transform and Runge-Kutta algorithms. Owing to the instabilities of the vacuum and of the stationary cw modes, noise is amplified and chaotically generates unstable accelerating pulses [see Figs. 4(a) and 5]. Note that the intensity of the pulses is generally higher for short times and smaller for longer times. This general behavior follows from the influence of FCA, which is initially zero at $t \to -\infty$ and grows as time increases. Generation of FCs affects the pulse dynamics also via FCD, which is the sole crucial term responsible for the acceleration towards shorter times. MI continuously generates unstable dissipative solitons that play the role of the strange attractor of the chaotic system, bifurcating, collapsing, and creating other pulses due to their inherent instability. Note that in ND (see Fig. 5) MI develops over a longer scale than in AD [see Fig. 4(a)], as FC generation is solely responsible for MI in ND. The characteristic duration of the chaotically generated pulses can be analytically predicted as $\Delta\tau \simeq 2\pi|\Delta\Omega|^{-1}$, where $\Delta\Omega$ is the instability frequency window that can be calculated directly from Eq. (14). For $g = 1$ and $g_2 = 0.16$, the analytical predictions for the pulse durations are $\Delta\tau \sim 500$ fs in AD and $\Delta\tau \sim 1$ ps in ND, finding agreement with numerical simulations [see Figs. 4(a) and 5]. The temporal acceleration

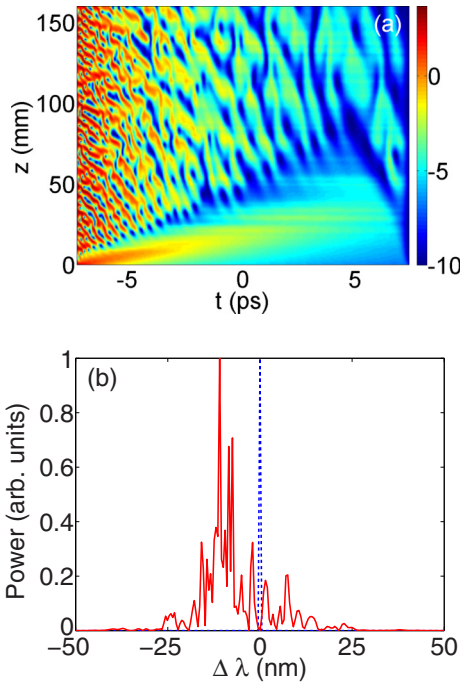

FIG. 4. (Color online) (a) Accelerating chaotic spatiotemporal dynamics in AD. The contour plot depicts the normalized optical power in logarithmic scale $10\log_{10}(|u|^2 + 0.1)$. (b) Output blue-shifted spectrum (red curve) and input spectrum (dashed blue curve). In the numerical simulation we used $g = 1$, $g_2 = 0.16$ and the parameters listed in Table I.

of the chaotically generated pulses is accompanied in the spectral domain by a blueshift of about 10 nm, as shown in Fig. 4(b). The main obstacle hampering further blueshifting is represented by the finite amplifying window of the gaining material. Thus, if other gaining media with larger spectral windows are used, a larger blueshift can be achieved.

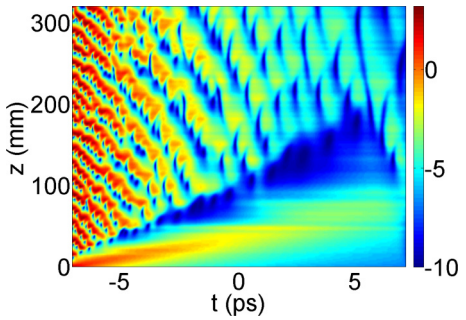

FIG. 5. (Color online) Accelerating chaotic spatiotemporal dynamics in ND. In the numerical simulation we used $g = 1$, $g_2 = 0.16$ and the parameters listed in Table I. The contour plot depicts the normalized optical power in logarithmic scale $10\log_{10}(|u|^2 + 0.1)$.

V. CONCLUSIONS

In conclusion, in this work we have investigated analytically and numerically the propagation dynamics of continuous waves in an amplifying silicon-based waveguide. We modeled optical propagation using a Ginzburg-Landau equation for the optical field coupled with a first-order differential equation accounting for the generation of free carriers. We have derived the stationary nonlinear cw mode of the system, and we have studied its stability against small perturbations, finding universal modulational instability in both anomalous and normal dispersion regimes. By numerically solving the governing equations we have observed an accelerating chaotic dynamics resulting from the inherent instabilities of the system. Our theoretical investigations have been focused on a realistically accessible setup, and our theoretical predictions can be experimentally verified.

ACKNOWLEDGMENTS

This research was funded by the German Max Planck Society for the Advancement of Science (MPG).

[1] B. Jalali, J. Lightwave Technol. **24**, 4600 (2006).
[2] R. Soref, IEEE J. Sel. Top. Quantum Electron. **12**, 1678 (2006).
[3] R. Soref, Nat. Photonics **4**, 495 (2010).
[4] P. Cheben, D.-X. Xu, S. Janz, and A. Densmore, Opt. Express **14**, 4695 (2006).
[5] J. Leuthold, C. Koos, and W. Freude, Nat. Photonics **4**, 535 (2010).
[6] L. Yin and G. P. Agrawal, Opt. Lett. **32**, 2031 (2007).
[7] Q. Lin, O. J. Painter, and G. P. Agrawal, Opt. Express **15**, 16604 (2007).
[8] C. A. Husko, S. Combrié, P. Colman, J. Zheng, A. De Rossi, and C. W. Wong, Sci. Rep. **3**, 1100 (2013).
[9] M. F. Saleh, W. Chang, P. Hölzer, A. Nazarkin, J. C. Travers, N. Y. Joly, P. St. J. Russell, and F. Biancalana, Phys. Rev. Lett. **107**, 203902 (2011).
[10] M. F. Saleh, W. Chang, J. C. Travers, P. St. J. Russell, and F. Biancalana, Phys. Rev. Lett. **109**, 113902 (2012).
[11] P. Hölzer, W. Chang, J. C. Travers, A. Nazarkin, J. Nold, N. Y. Joly, M. F. Saleh, F. Biancalana, and P. St. J. Russell, Phys. Rev. Lett. **107**, 203901 (2011).
[12] C. Koos, P. Vorreau, T. Vallaitis, P. Dumon, W. Bogaerts, R. Beats, B. Esembeson, I. Biaggio, T. Michinobu, F. Diederich, W. Freude, and J. Leuthold, Nat. Photonics **3**, 216 (2009).
[13] A. W. Fang, H. Park, Y. Kuo, R. Jones, O. Cohen, D. Liang, O. Raday, M. N. Sysak, M. J. Paniccia, and J. E. Bowers, Mater. Today **10**, 28 (2007).
[14] K. Wörhoff, J. D. B. Bredley, F. Ay, D. Geskus, T. P. Blauwendraat, and M. Pollnau, IEEE J. Quantum Electron. **45**, 454 (2009).
[15] L. Agazzi, J. Bradley, M. Dijkstra, F. Ay, G. Roelkens, R. Baets, K. Wörhoff, and M. Pollnau, Opt. Express **18**, 27703 (2010).
[16] N. Akhmediev and A. Ankiewicz, *Dissipative Solitons*, Lecture Notes in Physics, Vol. 661 (Springer, Berlin, 2005).

[17] I. S. Aranson and L. Kramer, Rev. Mod. Phys. **74**, 99 (2002).
[18] S. Kishiba, S. Toh, and T. Kawahara, Phys. D (Amsterdam, Neth.) **54**, 43 (1991).
[19] W. van Saarloos and P. C. Hohenberg, Phys. D (Amsterdam, Neth.) **56**, 303 (1992).
[20] G. P. Agrawal, *Nonlinear Fiber Optics*, 4th ed. (Academic, San Diego, 2008).
[21] N. R. Pereira and L. Stenflo, Phys. Fluids **20**, 1733 (1977).
[22] S. Roy, A. Marini, and F. Biancalana, Phys. Rev. A **87**, 065803 (2013).
[23] C. Gmachl, D. L. Sivco, R. Colombelli, F. Capasso, and A. Y. Cho, Nature (London) **415**, 883 (2002).
[24] COMSOL, version 3.5, http://www.comsol.co.in/.
[25] G. P. Agrawal, Phys. Rev. A **44**, 7493 (1991).
[26] A. Marini and D. V. Skryabin, Phys. Rev. A **81**, 033850 (2010).
[27] A. Marini, R. Hartley, A. V. Gorbach, and D. V. Skryabin, Phys. Rev. A **84**, 063839 (2011).
[28] D. V. Skryabin, A. V. Gorbach, and A. Marini, J. Opt. Soc. Am. B **28**, 109 (2011).
[29] I.-W. Hsieh, X. Chen, J. I. Dadap, N. C. Panoiu, R. M. Osgood, Jr., S. J. McNab, and Y. A. Vlasov, Opt. Express **14**, 12380 (2006).
[30] M. Dinu, F. Quochi, and H. Garcia, Appl. Phys. Lett. **82**, 2954 (2003).
[31] H. Rong, A. Liu, R. Nicolaescu, and M. Paniccia, Appl. Phys. Lett. **85**, 2196 (2004).
[32] Q. Lin, J. Zhang, G. Piredda, R. W. Boyd, P. M. Fauchet, and G. P. Agrawal, Appl. Phys. Lett. **91**, 021111 (2007).
[33] A. Marini, A. V. Gorbach, D. V. Skryabin, and A. V. Zayats, Opt. Lett. **34**, 2864 (2009).